Fast and Flexible

Tracking and Mitigating a Jamming Signal with an Adaptive Notch Filter

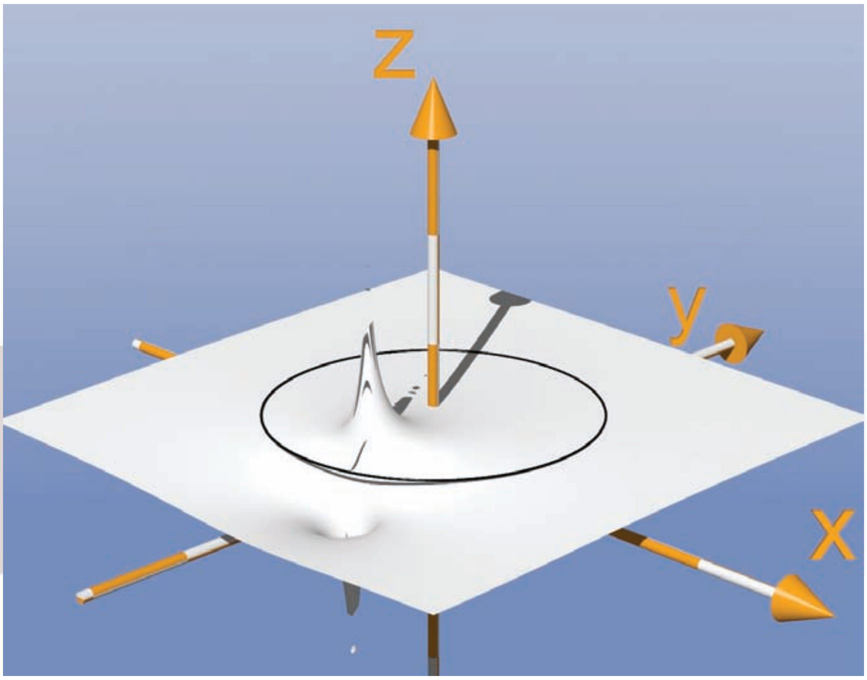

DANIELE BORIO, CILLIAN O'DRISCOLL, AND JOAQUIM FORTUNY
JOINT RESEARCH CENTER (JRC) OF THE EUROPEAN COMMISSION

The rise of inexpensive yet powerful GNSS jammers is driving numerous R&D efforts to find ways to thwart the use of such devices. Researchers at the European Commission Joint Research Center describe their use of an infinite impulse response adaptive notch filter to mitigate the effects of jamming.

GNSS jammers are small portable devices able to broadcast powerful disruptive signals in the GNSS bands. A jammer can overpower the much weaker GNSS signals and disrupt GNSS-based services in a geographical area with a radius of several kilometers. Despite the fact that the use of such devices is illegal in most countries, jammers can be easily purchased on the Internet and their rapid diffusion is becoming a serious threat to satellite navigation.

Several studies have analyzed the characteristics of the signals emitted by GNSS jammers. From the analyses, it emerges that jamming signals are usually characterized by linear frequency modulations: the instantaneous frequency of the signal sweeps a range of several megahertz in a few microseconds, affecting the entire GNSS band targeted by the device.

The fast variations of their instantaneous frequency make the design of mitigation techniques particularly challenging. Mitigation algorithms must track fast frequency variations and filter out the jamming signals without introducing significant distortions on the useful GNSS components. The design problem becomes even more challenging if only limited computational resources are available.

We have analyzed the ability of an adaptive notch filter to track fast frequency variations and mitigate a jamming signal. In this article, we begin by briefly describing the structure of the selected adaptive notch filter along with the adaptive criterion used to adjust the frequency of the filter notch.

When the adaptation parameters are properly selected, the notch filter can track the jamming signals and significantly extend the ability of a GNSS receiver to operate in the presence of jamming. Moreover, the frequency of the filter notch is an estimate of the instantaneous frequency of the jamming signal. Such information can be used to determine specific features of the jamming signal, which, in turn, can be used for jammer location using a time difference of arrival (TDOA) approach.

The capabilities of the notch filter are experimentally analyzed through

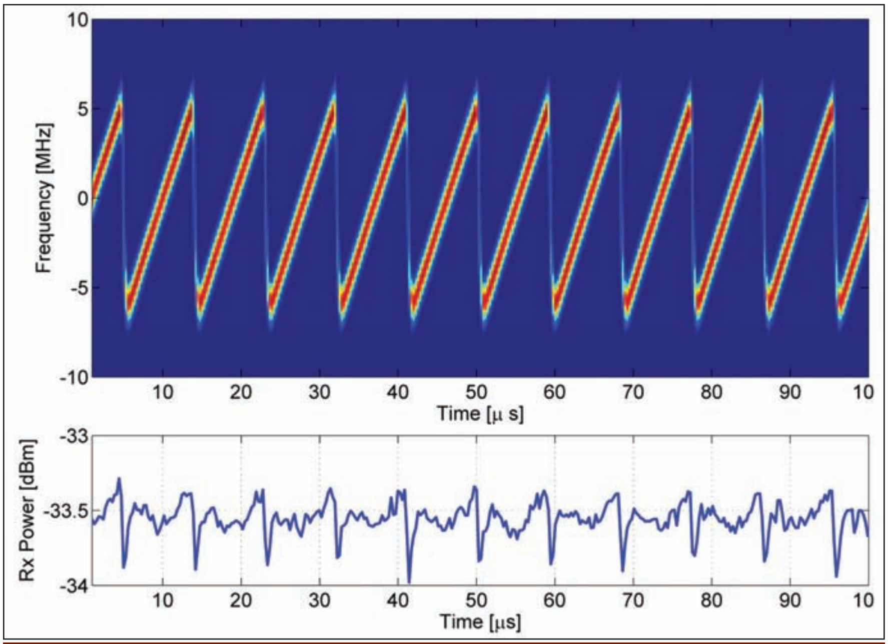

FIGURE 1 Time-frequency evolution of the signal transmitted by an in-car GPS jammer (instantaneous received signal power shown in the bottom part of the figure)

a series of experiments performed in a large anechoic chamber. The experiments employ a hardware simulator to broadcast GPS and Galileo signals and a real jammer to disrupt GNSS operations. The GNSS and interfering signals were recorded using an RF signal analyzer and analyzed in post-processing. We processed the collected samples using the selected adaptive notch filter and a custom GNSS software receiver developed in-house.

The use of mitigation techniques, such as notch filtering, significantly improves the performance of GNSS receivers, even in the presence of strong and fast-varying jamming signals. The presence of a pilot tone in the Galileo E1 signal enables pure phase-locked loop (PLL) tracking and makes the processing of Galileo signals more robust to jamming.

Adaptive Notch Filter

Several interference mitigation techniques have been described in the technical literature and are generally based on the interference cancellation principle. These techniques attempt to estimate the interference signal, which is subsequently removed from the input samples. For example, transform domain excision techniques at first project the input signal onto a domain where the inference signal assumes a sparse representation. (See the articles by J. Young *et alia* and M. Paonni *et alia*, referenced in the Additional Resources section near the end of this article.) The interference signal is then estimated from the most powerful coefficients of the transformed domain representation. The interfering signal is removed in the transformed domain, and the original signal representation is restored.

When the interfering signal is narrow band, discrete Fourier transform (DFT)-based frequency excision algorithms, described in the article by J. Young and J. Lehnert, are particularly effective. Transform domain excision techniques are, however, computationally demanding, and other mitigation approaches have been explored. For example, notch filters are particularly effective for removing continuous wave interference (CWI). M. Paonni *et alia*, cited in Additional Resources, considered the use of a digital notch filter for removing CWI, the center frequency of which was estimated using the fast Fourier transform (FFT) algorithm. Despite the efficiency of the FFT algorithm, this approach can result in a significant computational burden and alternative solutions should be considered.

The article by M. Jones described a finite impulse response (FIR) notch filter for removing unwanted CW components and highlighted the limitations of this type of filter. Thus, we adopted an infinite impulse response (IIR) structure and experimentally demonstrated its suitability for interference removal. In particular we considered the adaptive notch filter described in the article by D. Borio *et alia* listed in Additional Resources and investigated its suitability for mitigating the impact of a jamming signal.

This technique has been selected for its reduced computational requirements and for its good performance in the presence of CWI. Note that the notch filter under consideration has been extensively tested in the presence of CWI; however, its performance in the presence of frequency-modulated signals has not been assessed. Also, note that removing a jamming signal poses several challenges that derive from the swept nature of this type of interference. (For details, see the paper by R. H. Mitch *et alia*.)

Jamming signals are usually frequency modulated with a fast-varying center frequency. The time-frequency evolution of the signal transmitted by an in-car GPS jammer is provided as an example in **Figure 1**. The instantaneous center frequency of the jamming signal sweeps a frequency range of more than 10 megahertz in less than 10 microseconds. The adaptation criterion selected for estimating the center frequency of the jamming signal has to be sufficiently fast to track these frequency variations.

The notch filter considered in this work is characterized by the following transfer function (illustrated on the opening page of this article)

$$H_n(z)=\frac{1-z_0[n]z^{-1}}{1-k_\alpha z_0[n]z^{-1}} \qquad (1)$$

where k_α is the pole contraction factor and $z_0[n]$ is the filter zero. k_α controls the width of the notch introduced by the filter, whereas $z_0[n]$ determines the notch center frequency. Note that $z_0[n]$

is progressively adapted using a stochastic gradient approach described in the textbook by S. Haykin with the goal of minimizing the energy at the output of the filter. A thorough description of the adaptation algorithm can be found in the article by D. Borio *et alia*.

The notch filter is able to place a deep null in correspondence with the instantaneous frequency of narrow band interference and, if the zero adaptation parameters are properly chosen, to track the interference frequency variations. The energy of the filter output is minimized when the filter zero is placed in correspondence with the jammer instantaneous frequency

$$\frac{f_s}{2\pi} \angle z_0[n] \approx \Phi(nT_s) \quad (2)$$

where $\Phi(nT_s)$ is the jammer instantaneous frequency and $f_s = 1/T_s$ is the sampling frequency.

This implies that $z_0[n]$ can be used to estimate the instantaneous frequency of the interfering signal. The magnitude of $z_0[n]$ also strongly depends on the amplitude of the interfering signal. Indeed, $|z_0[n]|$ approaches one as the amplitude of the jamming signal increases. Thus, $|z_0[n]|$ can be used to detect the presence of interference, and the notch filter activates only if $|z_0[n]|$ passes a predefined threshold, T_z. A value of $T_z = 0.75$ was empirically selected for the tests described in the following section.

Experimental Setup and Testing

To test the capability of the adaptive notch filter to mitigate against a typical in-car jammer, we conducted several experiments in a large anechoic chamber at the Joint Research Centre (JRC) of the European Commission.

Figure 2 provides a view of the JRC anechoic chamber where the jamming tests were conducted. The anechoic chamber offers a completely controlled environment in which all sources of interference besides the jammer under test can be eliminated.

The experimental setup is similar to that employed to test the impact of LightSquared signals on GPS receivers (For details, see the article by P. Boulton *et alia* listed in Additional Resources). We used a simulator to provide a controlled GPS and Galileo constellation, with a static receiver operating under nominal open-sky conditions. The GNSS signals were broadcast from a right hand circular polarization (RHCP) antenna mounted on a movable sled on the ceiling of the chamber. A survey grade GNSS antenna was mounted inside the chamber, and the sled was positioned at a distance of approximately 10 meters from this antenna. The GNSS receiving antenna was connected via a splitter to a spectrum analyzer, an RF signal analyzer, and a commercial high sensitivity GPS receiver. **Table 1** lists the RF signal analyzer parameters.

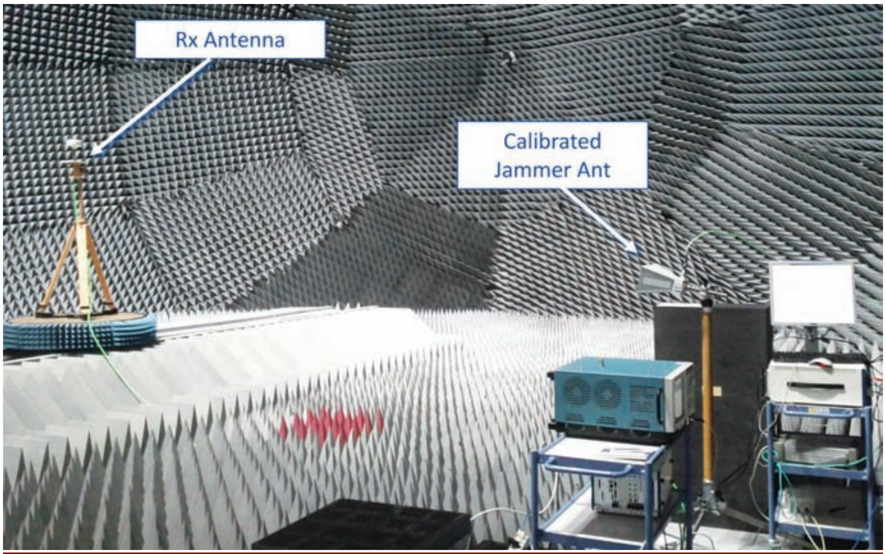

FIGURE 2 View of the JRC anechoic chamber where the jamming tests were conducted

To provide the source of jamming signals a commercially available (though illegal) in-car jammer was connected to a programmable power supply. We removed the jammer's antenna and connected the antenna port, via a programmable attenuator with up to 81 decibels of attenuation, to a calibrated standard gain horn antenna. This gain horn was positioned at approximately two meters from the GNSS receiving antenna.

The goal of this configuration was to permit variation of the total jammer power received at the antenna. Unfortunately, the jammer itself is very poorly shielded; so, a significant amount of the interfering power seen by the receiver was found to come directly from the body of the jammer, rather than through the antenna.

To minimize this effect, we exercised great care to shield the jammer as much as possible from the GNSS antenna. We placed the jammer body in an aluminum box, which was subsequently surrounded by RF absorbent material. The jammer body and the receiving GNSS antenna were separated by approximately 15 meters, thereby ensuring approximately 60 decibels of free space path loss.

The experiment was controlled via a PXI controller, which generated synchronous triggers for the RF data collection and simulator signal generation, controlled the power supplied to the jammer, and updated the attenuation settings according to a desired profile. All events (trigger generation, jammer power on/off, attenuation setting) were time stamped using an on-board timing module. The commercial receiver was configured to log raw GPS measurements including carrier-to-noise (C/N_0) values.

Parameter	Value
Center Frequency	1575.42 MHz
Sampling Rate	10 megahertz
Sample Type	Complex
Bits Per Sample	16
Bandwidth	≈ 10 megahertz

TABLE 1. Down converter/digitizer parameters

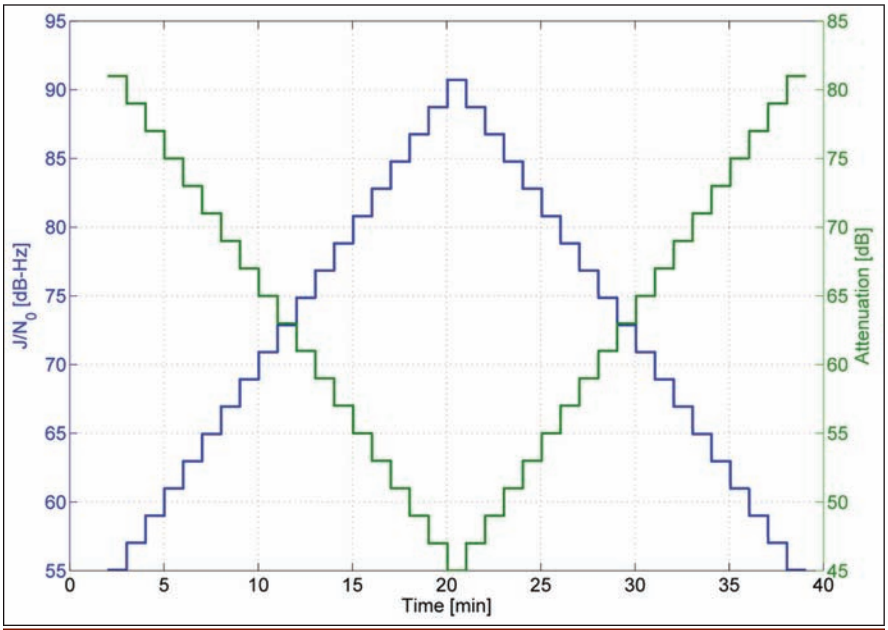

FIGURE 3 Attenuation profile applied to the jammer signal and calibrated J/N0 adopted for the experiment

The experimental procedure involved two trials, each lasting approximately 40 minutes. In the first trial, the simulator and data collection equipment were both enabled, but the jammer remained powered off. In the second trial, the same scenario was generated in the simulator, the data collection equipment was enabled and, after a period of three minutes, the jammer was powered on.

We initially set the attenuation to its maximum value of 81 decibels. We subsequently reduced this in two-decibel decrements to a minimum value of 45 decibels. We maintained each level for a period of 60 seconds. Finally, we again increased the attenuation in two-decibel increments to its maximum value. **Figure 3** presents this attenuation profile.

We performed a calibration procedure whereby the total received jammer power at the output of the active GNSS receiving antenna was measured using a calibrated spectrum analyzer while the attenuation level was varied. Further, the total noise power was measured in the same 12-megahertz bandwidth with the jammer switched off. This permitted the computation of the received jammer-to-noise density power ratio (J/N_0) as a function of the attenuator setting.

Figure 3 also shows the calibrated J/N_0 at the output of the active GNSS antenna as a function of time. The analysis provided in the next section is conducted as a function of the J/N_0.

Sample Results

This section provides sample results obtained using the adaptive notch filter described earlier. In particular, the loss in C/N_0 experienced by the GPS and Galileo software receivers used for analysis is experimentally determined as a function of the J/N_0.

The adaptive notch filter is used to reduce the C/N_0 loss. **Figure 4** shows the loss in C/N_0 experienced in the presence of the jammer as a function of J/N_0. The first curve arises from software receiver processing of the GPS signals, the second plot from software receiver processing of the Galileo signals, and the third from the commercial high sensitivity receiver that processed only the GPS signals.

Note the small difference between the GPS and Galileo results. This is to be expected due to the wideband nature of the jammer. In fact, for both GPS and Galileo processing the jammer is effectively averaged over many chirp periods, thereby giving it the appearance of a broadband (white) noise source. The one difference between the GPS and Galileo signals is that the tracking threshold of the Galileo signals is approximately six decibels lower than that for the GPS signals. This is due to the use of a pure PLL processing strategy using only the E1C (pilot) component of the Galileo signal.

The other interesting point to note from Figure 4 is that the commercial receiver exhibits better resilience against the jammer. This is most likely due to

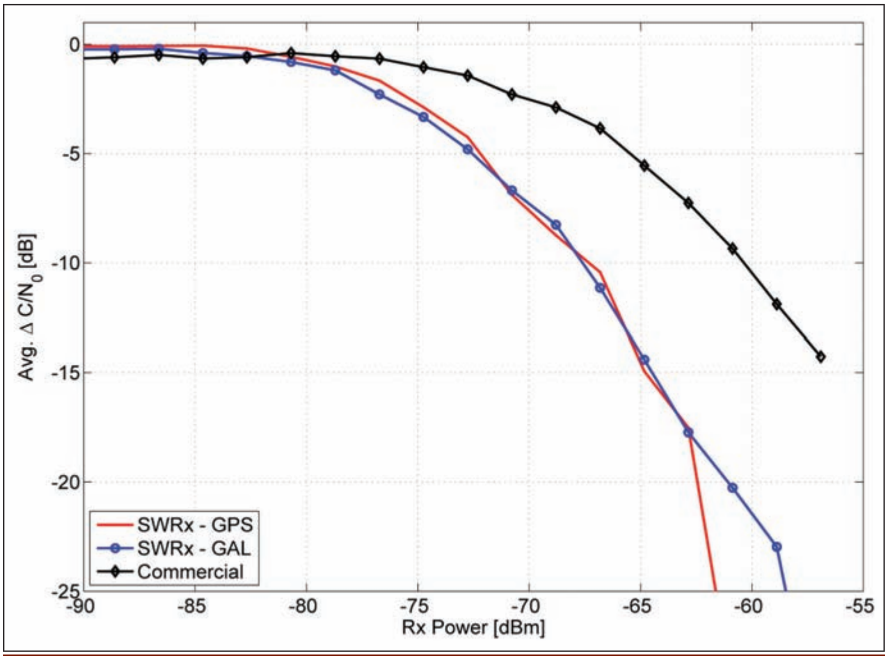

FIGURE 4 Average C/N_0 loss vs J/N_0 for: a) software receiver processing of GPS; b) software receiver processing of Galileo; and c) a commercial High Sensitivity GPS receiver.

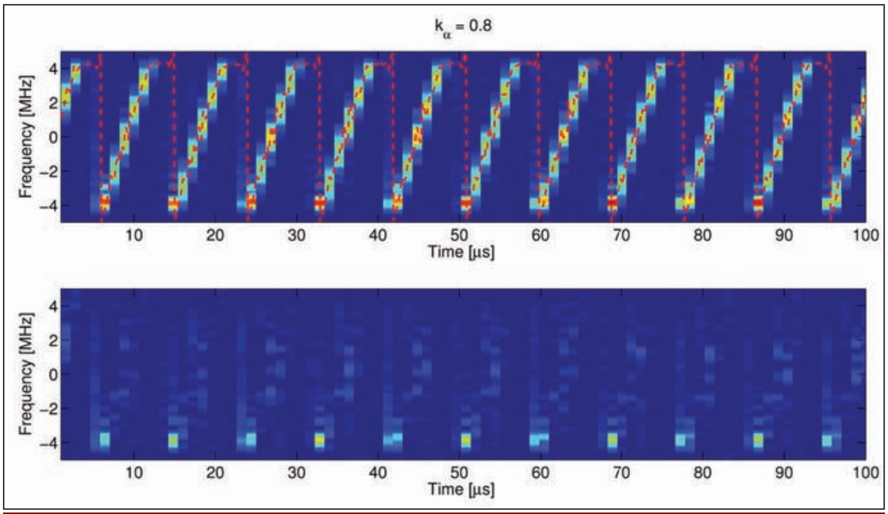

FIGURE 5 Time-frequency evolution of the received and notched ($k_\alpha = 0.8$) signals. The top plot shows the raw data with the estimated interference frequency obtained from the notch filter superimposed in red. The bottom plot shows the filtered data.

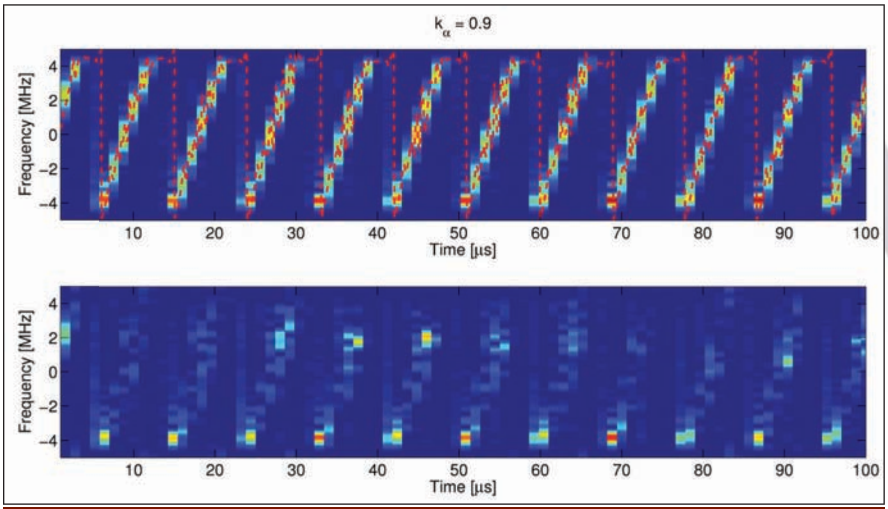

FIGURE.6 Time-frequency evolution of the received and notched ($k_\alpha = 0.9$) signals. The top plot shows the raw data with the estimated interference frequency obtained from the notch filter superimposed in red. The bottom plot shows the filtered data.

a narrower front-end bandwidth in the commercial receiver, although this cannot be confirmed because the receiver manufacturer does not provide this information.

From the time-frequency evolution of the jamming signal used for the experiment and shown in Figure 1, it emerges that the bandwidth of the jamming component is approximately 10 megahertz. If the commercial receiver had a smaller bandwidth, then it would effectively filter out some of the jammer power, thereby improving its performance with respect to the software receiver results.

Figure 4 provides an indication of the performance degradation caused by a jamming signal when no mitigation technique is employed. The notch filter is expected to improve the receiver performance. The improvement depends on the filter parameters and their ability to track the jammer's rapid frequency variation.

Two configurations of the adaptive notch filter were tested: $k_\alpha = 0.8$ and $k_\alpha = 0.9$. The first case has a smaller contraction factor and, hence, a wider notch than the latter.

The adaptive step size of the stochastic gradient algorithm was tuned for the jammer under consideration. (The adaptation of the filter zero must be fast to track the frequency variations of the jammer's chirp signal.) In each case the magnitude of the zero of the notch filter was used as a detector for interference. We chose a threshold of 0.75 so that when the amplitude of the zero was greater than this threshold, the notch filter was enabled and the receiver processed this filtered data. Otherwise the receiver processed the raw data collected from the antenna.

Figure 5 and **Figure 6** illustrate the results of the filtering for the two cases. In these plots, the upper portion shows the time evolution of the frequency content of the raw data, with the frequency estimate of the notch filter superimposed as a dashed red line. The lower plots show the time evolution of the frequency content of the filtered data. From these lower plots the wider notch appears to do a better job of removing the jammer signal. On the other hand, this will also result in a greater reduction of the useful signal power.

The effect of the notch filter on the reception of GNSS signals in terms of the C/N_0 degradation is illustrated in **Figure 7** and **Figure 8** for Galileo and GPS signals, respectively. Again, the difference between the impact on GPS and Galileo signals is slight, due to the wideband nature of the interferer. On the other hand, the benefit of the notch filter is clear in both figures. The sidebar, "Track the Jamming Signal," provides access to data and tools with which readers can test different configurations of the notch filters themselves.

Interestingly, it appears that two limiting curves exist, one for the case of no filtering and one for the case where a notch filter is applied. The variation in the contraction factor (over the range considered) has little effect on the C/N_0 effectively measured by the GPS and Galileo software receivers.

The separation between the two curves is approximately five decibels, i.e., the receiver that applies the notch filter experiences approximately five decibels less C/N_0 loss than an unprotected receiver for the same J/N_0. Of course, we

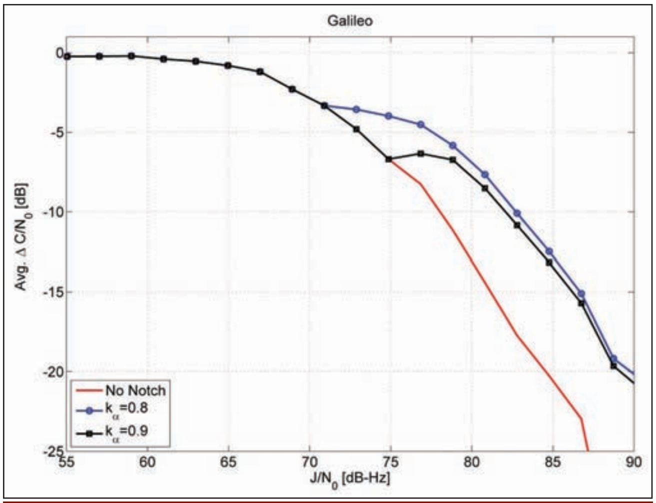

FIGURE 7 Average Galileo C/N_0 loss vs J/N_0 for: a) no notch filtering; b) notch filtering with k_α = 0.8; and c) k_α = 0.9

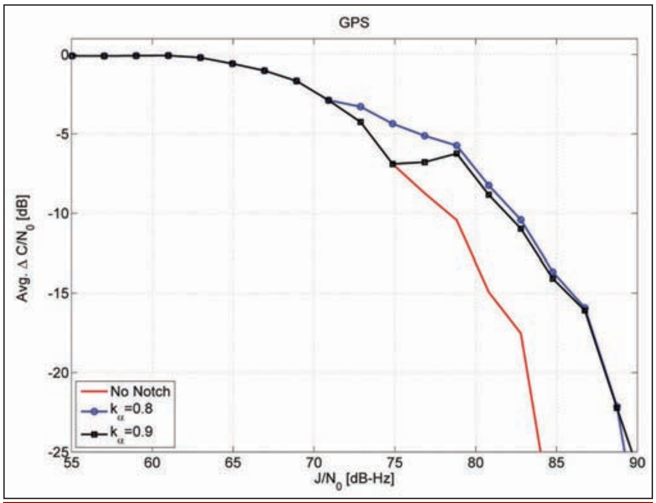

FIGURE 8 Average GPS C/N_0 loss vs J/N_0 for: a) no notch filtering; b) notch filtering with k_α = 0.8; and c) k_α = 0.9

must remember that this result applies for the data collection system considered in this test, which consists of a 14-bit analog-to-digital converter (ADC) with no automatic gain control (AGC). In commercially available receivers with a limited number of bits for signal quantization the non-linear losses due to the combination of these two front-end components will likely lead to additional losses.

Conclusion

We have proposed an IIR adaptive notch filter as an easy means to implement mitigation technique for chirp signals typical of the type of commercially available jammers that have become ever more present in recent years. A simple stochastic gradient adaptation algorithm was implemented, with an associated simple interference detection scheme. Our analysis showed that, for a receiver with sufficient dynamic range, the proposed technique leads to an improvement of approximately five decibels in terms of effective C/N_0.

We tested the proposed scheme on data collected from a low-cost commercial jammer in a large anechoic chamber. We used a software receiver to process both GPS and Galileo signals. The broadband nature of the chirp signal means that its effect on GNSS signal processing is similar to an increase in the thermal noise floor. Hence, the impact is very similar on both GPS and Galileo receivers. On the other hand, the chirp signal is instantaneously narrowband, a feature that is exploited by the use of a notch filter with a highly dynamic response to variations in the frequency of the interferer.

Acknowledgment

This study is mainly based on the paper “GNSS Jammers: Effects and Countermeasures” presented by the authors at the Satellite Navigation Technologies and European Workshop on GNSS Signals and Signal Processing, (NAVITEC), December 2012.

Additional Resources

[1] Borio, D., Camoriano, L., and Lo Presti, L., “Two-pole and Multi-pole Notch Filters: A Computationally Effective Solution for GNSS Interference Detection and Mitigation,” *IEEE Systems Journal,* Vol. 2, No. 1, pp. 38–47, March 2008

[2] Boulton, P., Borsato, R., and Judge, K., “GPS Interference Testing, Lab, Live, and LightSquared,” *Inside GNSS,* pp. 32-45, July/August 2011

[3] Haykin, S., *Adaptive Filter Theory,* 4th ed., Prentice Hall, September 2001

[4] Jones, M., “The Civilian Battlefield, Protecting GNSS Receivers from Interference and Jamming,” *Inside GNSS,* pp. 40-49, March/April 2011

[5] Mitch, R. H., Dougherty, R. C., Psiaki, M. L., Powell, S. P., O’Hanlon, B. W., Bhatti, J. A., and Humphreys, T. E., “Signal Characteristics of Civil GPS Jammers,” *Proceedings of the 24th International Technical Meeting of the Satellite Division of The Institute of Navigation (ION GNSS 2011),* Portland, OR, pp. 1907–1919, September 2011

[6] Paonni, M., Jang, J., Eissfeller, B., Wallner, S., Avila-Rodriguez, J. A., Samson, J., and Amarillo-Fernandez, F., “Wavelets and Notch Filtering, Innovative Techniques for Mitigating RF Interference,” *Inside GNSS,* pp. 54 – 62, January/February 2001

[7] Young, J. and Lehnert, J., “Analysis of DFT-based Frequency Excision Algorithms for Direct Sequence Spread-Spectrum Communications,” *IEEE Transactions on Communications,* Vol. 46, No. 8, pp. 1076 –1087, August 1998

Manufacturers

The experiments presented used a GSS8800 hardware simulator from **Spirent Communications,** Paignton, UK, adapted for broadcasting GPS and Galileo signals, and a real jammer used to disrupt GNSS operations. The GNSS and interfering signals were recorded using an NI PXI-5663 RF signal analyzer from **National Instruments Corporation**, Austin, Texas USA. The PXI controller was a National Instruments Timing Module PXI-6682H. The high-sensitivity receiver used in the tests was the Lea-5T from **u-blox AG**, Thalwil, Switzerland

Authors

Daniele Borio received an M.S. degree in communications engineering from Politecnico di Torino, Italy, an M.S. degree in electronics engineering from ENSERG/INPG de Grenoble, France, and a doctoral degree in

Track the Jamming Signal

The following Matlab scripts, which can be downloaded from <http://www.insidegnss.com/special/download/201403-jamming.rar> or <http://www.insidegnss.com/special/download/201403-jamming.zip>, enable the interested reader to try out the notch filter and its parameters:

- **adaptivenotch.m:** implementation of the adaptive notch filter described in the article. The filter is implemented as a Matlab struct, which is progressively updated by the "adaptivenotch" function.
- **filterdata.m:** main file which reads the input samples, calls the adaptive notch filter to mitigate the impact of the jamming signal, and stores the samples processed to disk.
- **dumpToFile.m:** routine called by "filterdata.m" to store the filtered samples to disk.
- **RealDataAcquisition.m:** script which can be used to qualitatively evaluate the effects of notch filtering on the acquisition of GPS signals corrupted by a jamming component.
- **DftParallelCodePhaseAcquisition.m, GpsCaCode.m and ResampleCode.m:** additional functions called by "RealDataAcquisition" for acquiring GPS L1 C/A code signals.

A short dataset ("JammerData.bin") containing GPS and Galileo signals corrupted by a jamming component is also provided. The dataset has been extracted from the samples collected using the experimental setup detailed in the main article and characterized by the parameters in Table 1.

The improvement that can be obtained using the notch filter is qualitatively shown in Figure 9 where the cross-ambiguity function (CAF) used for detecting the presence of GNSS signals is provided.

The notch filter is able to effectively remove the jamming signal, thus allowing a more reliable detection. **Figure 9** shows the detection of a GPS L1 C/A signal (PRN 7). When no mitigation technique is used, the CAF is corrupted by interfering components that mask the presence of the useful signal, as clearly shown in Figure 9 a). The jamming components are removed in Figure 9 b) where the notch filter has been used to process the input samples.

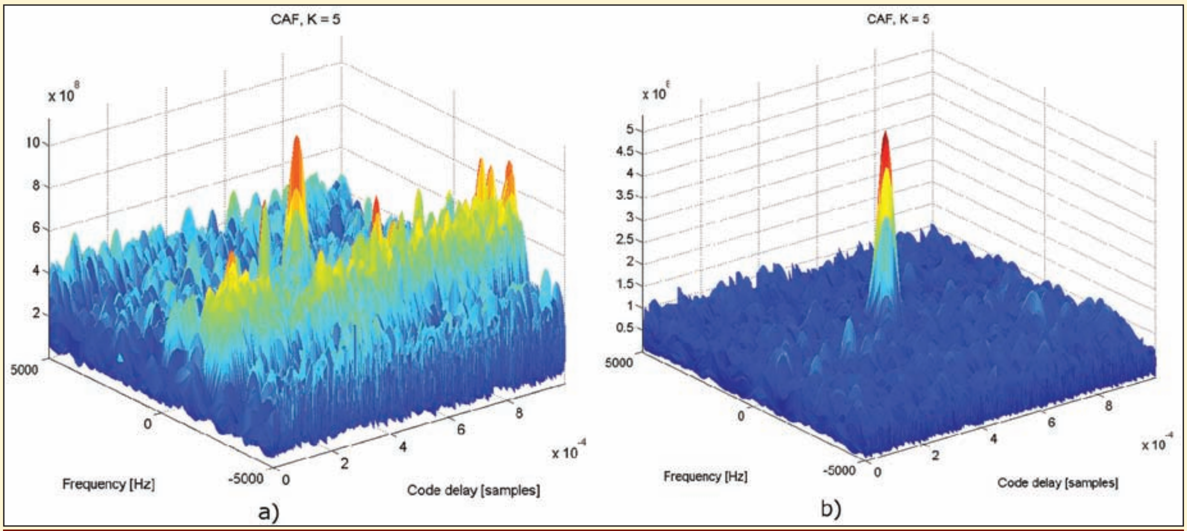

FIGURE 9 **Cross-ambiguity function evaluated using samples corrupted by a jamming signal. a) Original signal b) Signal processed using the adaptive notch filter. GPS L1 C/A signal from satellite PRN 7, five non-coherent integrations.**

electrical engineering from Politecnico di Torino. From January 2008 to September 2010 he was a senior research associate in the PLAN group of the University of Calgary, Canada. Since October 2010 he has been a research associate at the Joint Research Centre of the European Commission. His research interests include the fields of digital and wireless communications, location, and navigation.

Cillian O'Driscoll received his M.Eng.Sc. and Ph.D. degrees from the Department of Electrical and Electronic Engineering, University College Cork, Ireland. He was a senior research engineer with the Position, Location and Navigation (PLAN) group at the Department of Geomatics Engineering in the University of Calgary from 2007 to 2010. From January 2011 to December 2013, he served as scientific and policy officer of the European Commission. Since January 2014 he has been a research support officer at the University College Cork (UCC), Ireland. His research interests are in all areas of GNSS and of signal processing.

Joaquim Fortuny-Guasch received an engineering degree in telecommunications from the Technical University of Catalonia (UPC), Barcelona, Spain, and a Dr.-Ing. degree in electrical engineering from the Universität Karlsruhe (TH), Karlsruhe, Germany. Since 1993, he has been working for the Joint Research Centre (JRC) of the European Commission, Ispra, Italy, as senior scientific officer. He is the head of the European Microwave Signature Laboratory and leads the JRC research group on GNSS and wireless communications systems.

Prof.-Dr. Günter Hein serves as the editor of the Working Papers column. He is the head of the EGNOS and GNSS Evolution Program Department of the European Space Agency. Previously, he was a full professor and director of the Institute of Geodesy and Navigation at the Universität der Bundeswehr München. In 2002, he received the Johannes Kepler Award from the U.S. Institute of Navigation (ION) for "sustained and significant contributions" to satellite navigation. He is one of the inventors of the CBOC signal. IG